NATIONAL ADVISORY COMMITTEE FOR AERONAUTICS

NACA-TR-383

REPORT No. 383

ON THE THEORY OF WING SECTIONS WITH PARTICULAR REFERENCE TO THE LIFT DISTRIBUTION

By THEODORE THEODORSEN

1931

AERONAUTICAL SYMBOLS

1. FUNDAMENTAL AND DERIVED UNITS

	Symbol	Metric		English	
		Unit	Symbol	Unit	Symbol
Length	l	meter	m	foot (or mile)	ft. (or mi.)
Time	t	second	s	second (or hour)	sec. (or hr.)
Force	F	weight of one kilogram	kg	weight of one pound	lb.
Power	P	kg/m/s		horsepower	hp
Speed		km/h	k. p. h.	mi./hr.	m. p. h.
		m/s	m. p. s.	ft./sec.	f. p. s.

2. GENERAL SYMBOLS, ETC.

W, Weight $= mg$

g, Standard acceleration of gravity $= 9.80665$ m/s^2 $= 32.1740$ ft./sec.^{2}

m, Mass $= \frac{W}{g}$

ρ, Density (mass per unit volume).

Standard density of dry air, 0.12497 (kg-m^{-4} s^2) at 15° C. and 750 mm $= 0.002378$ (lb.-ft.$^{-4}$ sec.^{2}).

Specific weight of "standard" air, 1.2255 kg/m^3 $= 0.07651$ lb./ft.^{3}.

mk^2, Moment of inertia (indicate axis of the radius of gyration k, by proper subscript).

S, Area.

S_w, Wing area, etc.

G, Gap.

b, Span.

c, Chord.

$\frac{b^2}{S}$, Aspect ratio.

μ, Coefficient of viscosity.

3. AERODYNAMICAL SYMBOLS

V, True air speed.

q, Dynamic (or impact) pressure $= \frac{1}{2}\rho V^2$.

L, Lift, absolute coefficient $C_L = \frac{L}{qS}$

D, Drag, absolute coefficient $C_D = \frac{D}{qS}$

D_o, Profile drag, absolute coefficient $C_{D_o} = \frac{D_o}{qS}$

D_i, Induced drag, absolute coefficient $C_{D_i} = \frac{D_i}{qS}$

D_p, Parasite drag, absolute coefficient $C_{D_p} = \frac{D_p}{qS}$

C, Cross-wind force, absolute coefficient $C_C = \frac{C}{qS}$

R, Resultant force.

i_w, Angle of setting of wings (relative to thrust line).

i_t, Angle of stabilizer setting (relative to thrust line).

Q, Resultant moment.

Ω, Resultant angular velocity.

$\rho\frac{Vl}{u}$, Reynolds Number, where l is a linear dimension.

e. g., for a model airfoil 3 in. chord, 100 mi./hr. normal pressure, at 15° C., the corresponding number is 234,000;

or for a model of 10 cm chord 40 m/s, the corresponding number is 274,000.

C_p, Center of pressure coefficient (ratio of distance of $c.\ p.$ from leading edge to chord length).

α, Angle of attack.

ϵ, Angle of downwash.

α_o, Angle of attack, infinite aspect ratio.

α_i, Angle of attack, induced.

α_a, Angle of attack, absolute.

(Measured from zero lift position.)

γ, Flight path angle.

REPORT No. 383

ON THE THEORY OF WING SECTIONS WITH PARTICULAR REFERENCE TO THE LIFT DISTRIBUTION

By THEODORE THEODORSEN
Langley Memorial Aeronautical Laboratory

NATIONAL ADVISORY COMMITTEE FOR AERONAUTICS

NAVY BUILDING, WASHINGTON, D. C.

(An independent Government establishment, created by act of Congress approved March 3, 1915, for the supervision and direction of the scientific study of the problems of flight. Its membership was increased to 15 by act approved March 2, 1929 (Public, No. 908, 70th Congress). It consists of members who are appointed by the President, all of whom serve as such without compensation.)

EXECUTIVE COMMITTEE

REPORT No. 383

ON THE THEORY OF WING SECTIONS WITH PARTICULAR REFERENCE TO THE LIFT DISTRIBUTION

By THEODORE THEODORSEN

SUMMARY

This paper gives a simple and exact method of calculating the lift distribution on thin wing sections. The most essential feature of the new theory is the introduction of an "ideal angle of attack," this angle being defined as that at which the flow enters the leading edge smoothly or, more precisely, as the angle of attack at which the lift at the leading edge equals zero. The lift distribution at this particular angle is shown to be a characteristic property of the section and has been termed the "basic distribution." It is shown that the lift of a wing section may always be considered to consist of (a) the basic distribution and (b) the additional distribution, where the latter is independent of the mean camber line and thus identical for all thin sections. The specific reason for the poor aerodynamic qualities of thin wing sections is pointed out as being due to the fact that the additional lif tin potential flow becomes infinite at the leading edge.

The theory is in consequence adapted to describe some of the properties of actual wing sections. It is established that the essential parameter occurring in this analysis is the radius of curvature at the leading edge. The location and magnitude of the maximum lift intensity is determined. It is further pointed out that the actual slope of the lift curve is dependent on this parameter.

The theoretical lift distribution is compared with the distribution obtained by direct measurement on a number of the more conventional wing sections. The results check satisfactorily and may be considered as a confirmation of the validity of the theory.

The new theory will be of value in the further improvements of airplane wings. It is pointed out that airplanes should be operated near the ideal angle of attack. The theory will also be of use in calculating the structural strength of wing sections.

INTRODUCTION

The existing theory for thin wing sections leads, in general, to an infinite velocity around the front edge. The condition is shown exaggerated in Figure 1. To avoid this inaccuracy a new condition has to be introduced. This is the requirement of a smooth flow around the front edge. It will be noticed that this is in analogy with the well-known Kutta condition for the rear edge. The new developments lead directly to the establishment of an angle of maximum "entrance efficiency."

It has been found possible to extend the theory also to thick or actual wing sections. The most important parameter in this analysis is the radius of curvature at the leading edge.

Even with the advances made in the field of experimental aerodynamics, the mere knowledge of the expected total lift and moment of a wing section furnishes but a poor guidance, if any at all.

The usual theory of wing sections is only capable of giving the total lift and the total moment on a wing section, the new gives also the pressure distribution.

The main object of the study was to establish the pressure or lift distribution on the actual airfoil. On

FIGURE 1

introducing the requirement of a smooth flow at the entrance edge the author has been able to determine the theoretical pressure distribution on a thin wing section. This distribution is of interest in the study of the properties of actual wing sections of similar basic shape. This distribution occurs only at a given angle of attack. This angle, which is a given characteristic of each airfoil, has been termed the ideal angle of attack.

It is shown that the lift distribution may be considered to consist of the basic distribution at the ideal angle plus a given function multiplied by the angle of attack as measured from this ideal angle.

This function has been determined theoretically for actual wing sections.

Considerable simplification in the method and a resulting greater applicability of the theoretical deductions to actual testing have been obtained. The theoretical prediction of the effect of changes in the airfoil has, in particular, been simplified.

The new theory has been successfully applied to some of the more frequently used wing sections for which test data were available. For this work we feel greatly indebted to Mr. R. M. Pinkerton of the Langley Memorial Aeronautical Laboratory.

It is on a precise knowledge of the expected individual rôles played by each element in their contribution to the whole that the road to future developments must be based. As usual, it may be said that no comprehension of the effect of arbitrary changes may be arrived at without the guidance of the theory. It is the exclusive merit of a rigid theory to limit the number of possible variables to a reasonable number, thus eliminating unnecessary experimenting, and of guiding the work into definite channels from which ultimately the useful facts are bound to emanate.

REPORT No. 383

ON THE THEORY OF WING SECTIONS WITH PARTICULAR REFERENCE TO THE LIFT DISTRIBUTION

PART I

GENERAL

In order to avoid any repetition of the theory of the airfoil as it exists at the present time, we will refer

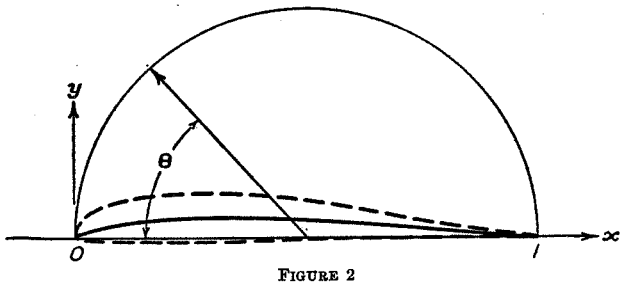

FIGURE 2

exclusively to the works of Glauert as given in Reference 1.

We will in consequence adopt the nomenclature used by him throughout this study.[1] The system of coordinates is shown in Figure 2.

Glauert's work is in agreement with the principles developed by Max M. Munk.

CALCULATION OF THE ANGULAR DISTORTION

The angular distortion ϵ plays an important rôle in the following theory. In fact, if the ϵ curve is known for a wing section, all the characteristics are obtained with ease.

Just in the same manner as an airfoil is considered as a distorted straight line, its almost circular image may be considered as a distorted circle.

The angular distortion is given by $\epsilon = -\Sigma A_n \cos n\theta$; the radial distortion by $r = \Sigma A_n \sin n\theta$ where

$$A_n \text{ is given as } \frac{2}{\pi}\int_0^\pi r \sin n\theta \, \mathrm{d}\theta.*$$

We may then write

$$\epsilon_x = -\frac{2}{\pi}\Sigma \cos n\theta_x \int_0^\pi r \sin n\theta \, \mathrm{d}\theta$$

where the symbols θ_x and θ are used in order to distinguish between the two different kinds of variables.

This expression can easily be transformed to

$$\epsilon_x = -\frac{1}{\pi}\sum_n \int_0^\pi r[\sin n(\theta-\theta_x) + \sin n(\theta+\theta_x)]\mathrm{d}\theta. \quad \text{I}$$

In order to develop this integral further we write

$$\Sigma \sin nx = +\sum_n \frac{e^{inx}-e^{-inx}}{2i} = \frac{1}{2i}\Sigma(e^{inx}-e^{-inx})$$

$$= -\frac{1}{2}i\,\Sigma(e^{inx}-e^{-inx})$$

Let

$$\Sigma e^{inx} = e^{ix}+e^{2ix}+e^{3ix}+ \ \ldots \ = S.$$

This series is not convergent and its value is perfectly indeterminate.

This difficulty can be avoided, however, by the following stratagem. We write

$$S = e^{ix}+e^{2ix}+e^{3ix}+ \ \ldots \ e^{n-1x}$$

and

$$-Se^{ix} = -e^{2ix}-e^{3ix} \ \ldots \ -e^{n-1x}-e^{nx}$$

By addition

$$S(1-e^{ix}) = e^{ix}-e^{inx} \text{ or } S = \frac{e^{ix}-e^{inx}}{1-e^{ix}}$$

Similarly

$$\Sigma_n e^{-inx} = S_1 = \frac{e^{-ix}-e^{-inx}}{1-e^{-ix}}$$

Then

$$S-S_1 = \frac{e^{ix}-e^{inx}}{1-e^{ix}} - \frac{e^{-ix}-e^{-inx}}{1-e^{-ix}}$$

$$= \frac{e^{ix}-e^{inx}+1-e^{-i(n-1)x}}{1-e^{ix}}$$

$$= \frac{1+e^{ix}}{1-e^{ix}} - \frac{e^{inx}+e^{-i(n-1)x}}{1-e^{ix}}$$

and

$$\Sigma \sin nx = -\frac{1}{2}i\left(\frac{1+e^{ix}}{1-e^{ix}} - \psi\right)$$

where

$$\psi = \frac{e^{inx}+e^{-i(n-1)x}}{1-e^{ix}}$$

$$\Sigma \sin nx = -\frac{1}{2}i\left(\frac{e^{-\frac{1}{2}ix}+e^{\frac{1}{2}ix}}{e^{-\frac{1}{2}ix}-e^{\frac{1}{2}ix}} - \psi\right)$$

$$= \frac{1}{2}\cot\frac{x}{2} + \frac{1}{2}i\,\psi$$

From equation I

$$\epsilon_x = -\frac{1}{2\pi}\int_0^\pi r\left(\cot\frac{\theta+\theta_x}{2} + \cot\frac{\theta-\theta_x}{2} + i\psi_1 + i\psi_2\right)\mathrm{d}\,\theta.$$

[1] With the exception that ϵ_0 has been replaced by the more logical ϵ_1 at $x=1$ and with ϵ_0 corresponding to $x=0$, and the lift coefficient C_L is used instead of the British $K_L(C_L=2K_L)$. Nondimensional equations are used throughout the report.

* *(Reference 1, p. 2.)*

The functions $i\psi_1$ and $i\psi_2$ containing the arguments $\frac{\theta+\theta_x}{2}$ and $\frac{\theta-\theta_x}{2}$, respectively, have infinitely high periods and thus furnish nothing to the value of the integral. Therefore

$$\epsilon_x = -\frac{1}{2\pi}\int_0^\pi r\left(\cot\frac{\theta+\theta_x}{2}+\cot\frac{\theta-\theta_x}{2}\right)\mathrm{d}\,\theta. \qquad \text{II}$$

In order to separate the independent variables θ and θ_x, we write

$$\cot\left(\frac{\theta}{2}\pm\frac{\theta_x}{2}\right)=\frac{\left(\cot\frac{\theta}{2}\cot\frac{\theta_x}{2}\mp 1\right)}{\left(\cot\frac{\theta_x}{2}\pm\cot\frac{\theta}{2}\right)}=\frac{(AB\mp 1)}{(\pm A+B)}$$

where $A=\cot\frac{\theta}{2}$ and $B=\cot\frac{\theta_x}{2}$. Then

$$\cot\left(\frac{\theta}{2}+\frac{\theta_x}{2}\right)+\cot\left(\frac{\theta}{2}-\frac{\theta_x}{2}\right)$$
$$=\frac{AB-1}{A+B}+\frac{AB+1}{-A+B}$$
$$=\frac{(AB-1)\ (-A+B)+(A+B)\ (AB+1)}{B^2-A^2}$$
$$=\frac{2A(1+B^2)}{B^2-A^2}$$

and

$$\cot\left(\frac{\theta}{2}+\frac{\theta_x}{2}\right)+\cot\left(\frac{\theta}{2}-\frac{\theta_x}{2}\right)=\frac{2\cot\frac{\theta}{2}\left(1+\cot^2\frac{\theta_x}{2}\right)}{\cot^2\frac{\theta_x}{2}-\cot^2\frac{\theta}{2}}$$

This gives

$$\epsilon_x=\frac{1}{\pi}\int_0^\pi r\,\frac{\cot\frac{\theta}{2}\left(1+\cot^2\frac{\theta_x}{2}\right)}{\cot^2\frac{\theta}{2}-\cot^2\frac{\theta_x}{2}}\,\mathrm{d}\,\theta. \qquad \text{III}$$

Using coordinates given as fractions of the chord with zero at the leading edge (Figure 2),

$$1-\cos\theta=2x \text{ and } \sin^2\theta=4x(1-x),$$

we obtain

$$\cot\frac{\theta}{2}=\frac{\sin\theta}{1-\cos\theta}=\frac{2\sqrt{x(1-x)}}{2x}=\sqrt{\frac{1}{x}-1}$$

also

$$r=\frac{2y^*}{\sin\theta} \text{ and } \mathrm{d}\theta=\frac{2\mathrm{d}x}{\sin\theta}.$$

Introduced in III, this gives

$$\epsilon_{x_1}=\frac{1}{\pi}\int_0^\pi r\mathrm{d}\theta\,\frac{\sqrt{\frac{1}{x}-1}\quad\left(\frac{1}{x_1}\right)}{\left(\frac{1}{x}-1\right)-\left(\frac{1}{x_1}-1\right)}$$
$$=\frac{1}{\pi}\int_0^\pi r\mathrm{d}\theta\,\frac{\sqrt{\frac{1}{x}-1}\quad\left(\frac{1}{x_1}\right)}{\frac{1}{x}-\frac{1}{x_1}}$$
$$=\frac{1}{\pi}\int_0^1 y\mathrm{d}x\,\frac{\sqrt{\frac{1}{x}-1}\quad\left(\frac{1}{x_1}\right)}{\left(\frac{1}{x}-\frac{1}{x_1}\right)x(1-x)}$$

and finally

$$\epsilon_{x_1}=\frac{1}{\pi}\int_0^{x=1}\frac{y\mathrm{d}x}{(x_1-x)\sqrt{x(1-x)}} \qquad \text{IV}$$

It is important to notice that the x-axis must coincide with the line joining the extremities of the mean camber line as indicated in Figure 2.

The integrand becomes infinite at the point $x=x_1$. The value of the integral is, however, finite.

Introducing $P=\frac{y}{\sqrt{x(1-x)}}$, we have

$$\epsilon_{x_1}=\frac{1}{\pi}\int_0^1\frac{P\mathrm{d}x}{x_1-x}$$

This relation may also be written

$$\epsilon_{x_1}=\frac{1}{\pi}\int_0^x\frac{P_x-P_{(2x_1-x)}}{x_1-x}\,\mathrm{d}x. \qquad \text{V}$$

That is, from the value P_x at x is subtracted the value $P_{(2x_1-x)}$ at the point $2x_1-x$, which is located the same distance from the point x_1, but in the opposite direction.

This integrand does not become infinite at any point $0<x<1$, and the integration can be performed for any profile.

The calculated ϵ-curves for three typical wing sections are shown in Figures 18, 19, and 20.

CALCULATION OF ϵ_0 AND ϵ_1

The calculation of ϵ_0 and ϵ_1 is more difficult, due to the fact that the integrand becomes infinite if the derivative y' is different from zero.

Let us calculate the contributions to ϵ_0 from the element between 0 and Δx where Δx is a very small quantity.

Assuming y to be a straight line between 0 and Δx, we observe that the contribution to the integral, equation IV, is

$$\Delta\epsilon_0=-\frac{1}{\pi}\int_0^{\Delta x}\frac{y'_{(0)}\mathrm{d}x}{\sqrt{x}}=\left[-\frac{2}{\pi}y'\sqrt{x}\right]_0^{\Delta x}=-\frac{2\Delta y}{\pi\sqrt{\Delta x}} \text{ and}$$

for $\Delta x=0.05$

$$\Delta\epsilon_0=-2.85y_{0.05} \qquad \text{VI}$$

If y is curved upwards between 0 and 0.05, the contribution to the integral is somewhat larger. Similarly we obtain $\Delta\epsilon_1=+2.85y_{0.95}$ as the contribution to ϵ_1 from the element adjacent to the rear edge.

GRAPHICAL EVALUATION OF ϵ_x

Plot the function P, see Figure 3. Construct the curve carefully near 0 and 1.

To find ϵ_{x_1} draw lines as shown in figure. It will be noticed that the integral

$$\epsilon_{x_1}=\frac{1}{\pi}\int_0^1\frac{P\mathrm{d}x}{x_1-x}$$

* (*Reference 1, p. 2.*)

also may be written

$$\epsilon_{x_1} = -\frac{1}{\pi}\int_0^{\infty} \tan \alpha \, dx \qquad \text{VII}$$

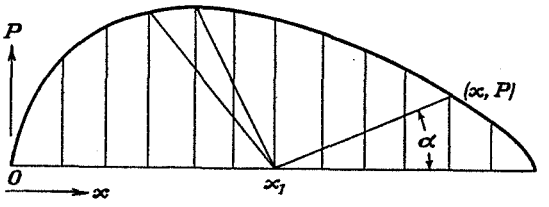

FIGURE 3

where α is the angle formed by a line drawn from $(x_1, 0)$ to (x, P) as indicated in Figure 3.

Infinite values of tan α are avoided by subtracting corresponding values of P as indicated above. This amounts to folding the area around x_1 and taking the integral for the resulting difference, Figure 4. Since P crosses the x axis at right angles, it will be noticed

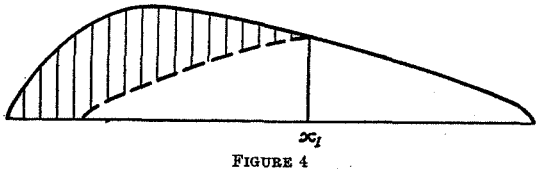

FIGURE 4

that ϵ_0 and ϵ_1 actually contain elements of infinite height. The area formed is, however, finite and can be obtained graphically or by the calculation shown above.

REPORT No. 383

ON THE THEORY OF WING SECTIONS WITH PARTICULAR REFERENCE TO THE LIFT DISTRIBUTION

PART II

ANALYSIS OF THE EXISTING THEORY

The nondimensional pressure P as given by Glauert may be written in the form

$$P=4(\alpha+\epsilon_1)\sqrt{\frac{1}{x}-1}+[4\frac{d}{dx}(\epsilon-\epsilon_1)\sqrt{x(1-x)}]$$

(from reference 1, p. 5) or

$$\frac{1}{4}P=(\alpha+\epsilon_1)\sqrt{\frac{1}{x}-1}-\frac{d}{dx}[(\epsilon_1-\epsilon)\sqrt{x(1-x)}.] \qquad \text{VIII}$$

(The function $\sqrt{x(1-x)}=R$ appears throughout the work and is given for convenience in Table I.)

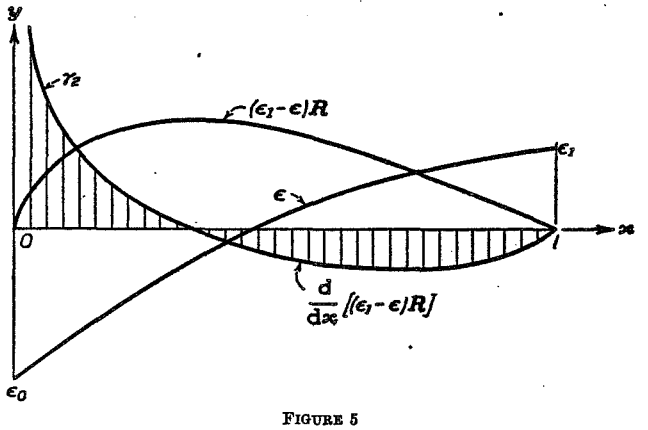

FIGURE 5

Now that we have actually been able to determine the value of the distortion ϵ, we are able to express P as a definite function of the position x.

This work will be taken up in Part III.

It is very interesting to notice that the second function $-\frac{d}{dx}[(\epsilon_1-\epsilon)\sqrt{x(1-x)}]$ is vital in determining the pressure distribution on the section, while it does not affect the total pressure or the lift of the wing.

$$\int_0^1 \frac{d}{dx}[(\epsilon-\epsilon_1)\sqrt{x(1-x)}]\,dx=0.$$

The integral is identically zero, Figure 5.

The total pressure on the wing is thus given by

$$4(\alpha+\epsilon_1)\int_0^1\sqrt{\frac{1}{x}-1}\,dx$$

where $\frac{1}{x}-1=\cot^2\frac{\alpha}{2}$ and $dx=\frac{1}{2}\sin\alpha d\alpha$

$$4(\alpha+\epsilon_1)\int_0^\pi \cot\frac{\alpha}{2}\sin\frac{\alpha}{2}\cos\frac{\alpha}{2}\,d\alpha$$

$$=4(\alpha+\epsilon_1)\int_0^\pi \cos^2\frac{\alpha}{2}\,d\alpha$$

$$=8(\alpha+\epsilon_1)\int_0^\pi \cos^2\frac{\alpha}{2}\,d\frac{\alpha}{2}$$

$$=8(\alpha+\epsilon_1)\left[\frac{1}{2}\frac{\alpha}{2}+\frac{1}{4}\sin\alpha\right]_0^\pi$$

$$=2(\alpha+\epsilon_1)\pi$$

which is the value of the absolute lift coefficient in accordance with this theory.

The expression $\frac{d}{dx}[(\epsilon_1-\epsilon)\sqrt{x(1-x)}]$ is entirely a function of the shape of the airfoil and is thus not altered with a change in the angle of attack.

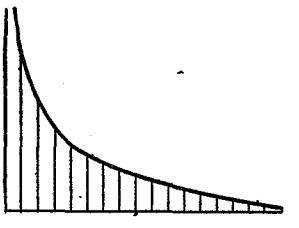

FIGURE 6

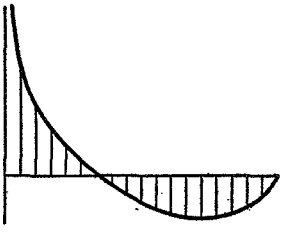

FIGURE 7

Let us express the equation

$$\frac{1}{4}P=(\alpha+\epsilon_1)\sqrt{\frac{1}{x}-1}-\frac{d}{dx}[(\epsilon_1-\epsilon)\sqrt{x(1-x)}] \text{ as}$$

$$\frac{1}{4}P=\gamma_1-\gamma_2$$

The distribution of γ_1 is indicated in Figure 6. It is infinite at the leading edge and zero at the trailing edge. The distribution of γ_2 is indicated approximately by Figure 7. The value of this function is also infinite and zero at the front and rear edge, respectively, but the net area equals zero.

For a point close to the front edge we are confronted with the actual determination of the value $\infty-\infty$ obtained by subtracting γ_2 from γ_1.

This quantity is determined as follows:
Let us write for a point close to the origin

$$\frac{1}{4} P_{\Delta x} = (\alpha + \epsilon_1) \sqrt{\frac{1}{\Delta x}} - \frac{d}{dx} [(\epsilon_1 - \epsilon) \sqrt{\Delta x}]$$

$$= (\alpha + \epsilon_1) \frac{1}{\sqrt{\Delta x}} - (\epsilon_1 - \epsilon) \frac{1}{2\sqrt{\Delta x}} + \sqrt{\Delta x} \frac{d\epsilon}{dx}$$

The last term $\sqrt{\Delta x} \frac{d\epsilon}{dx}$ is negligible compared with the other terms and therefore

$$\frac{1}{4} P_{\Delta x} = \frac{1}{\sqrt{\Delta x}} \left(\alpha + \frac{1}{2} \epsilon_1 + \frac{1}{2} \epsilon \right).$$

This pressure is zero only if $\epsilon_0 = -2\alpha - \epsilon_1$. In all other cases the pressure at the very edge is infinite, indicating that nonpermissible conditions are imposed by the theory. This relationship could have been expected. It is possible to show directly that the front stagnation point occurs at the angle $-2\alpha - \epsilon_1$.

In order to obtain smooth flow past the front edge of the infinitely thin airfoil it is necessary that the above relation be satisfied, that is

$$\epsilon_0 = -2\alpha - \epsilon_1. \qquad \text{IX}$$

It is noticed from the expression just developed for the pressure near the front edge that this requirement is actually a necessity in order to avoid infinite pressures at this point. We may even go a step further in stating that the existing theory of thin wing sections fails to give the true values of the lift and moment, except for the definite value of the angle of attack:

$$\alpha_I = -\frac{\epsilon_0 + \epsilon_1}{2} \qquad \text{X}$$

Let us call this the ideal angle of attack. In all other cases the usual theory leads to infinite pressure differences across the leading edge. The assumption of a noncompressible fluid, on which this theory is based, is obviously violated. The theory breaks down in a precise study of localized effects.

This angle plays in the aerodynamic theory of airfoils a rôle just as predominant as that of the entrance angle in the theory of turbines. While in the theory of turbines the question of entrance angles is completely settled, enough thought has probably not been given to the corresponding problem in aerodynamics.

DISCUSSION OF EXPRESSION FOR PRESSURE ON WING SECTION

Glauert gives as expression for the numerical value of the velocity around the airfoil:

$$q = V \left[1 + (\alpha + \epsilon \cot\theta + (\alpha + \epsilon_1) \operatorname{cosec}\theta + \frac{d\epsilon}{d\theta} \right]$$

(Reference I, equation 14). We will observe that near $\theta = \pi$ no difficulties are encountered, since the infinite factors actually will cancel each other at $\theta = \pi$ due to the Kutta condition.

As $\theta \to 0$ we run into difficulties. We obtain for a point $\theta = +\Delta\theta$,

$$q = V \left[1 + (\alpha + \epsilon_0) \frac{1}{\Delta\theta} + (\alpha + \epsilon_1) \frac{1}{\Delta\theta} + \frac{d\epsilon}{d\theta} \right]. \qquad \text{XI}$$

Glauert's method of calculating the pitching moment on the basis of equation 14 is not strictly permissible. The factor $[(\alpha + \epsilon) \cot\theta + (\alpha + \epsilon_1) \operatorname{cosec}\theta]$ can not be treated as a small quantity near the origin, and the squares and products of such large quantities can not be neglected as compared with unity.

We know the numerical value of the velocity can not become less than zero and the corresponding pressure not greater than $\frac{1}{2} \rho V^2$. There is also a limit to the maximum value of the velocity. This will not pass the sound velocity of the medium, and the greatest negative pressure is, in consequence, about one-half atmosphere.[2]

The difficulties are, however, dispensed with by introducing what we will call the front edge condition.

It will be noticed that if ϵ_0 happens to be equal to $-(2\alpha + \epsilon_1)$, there is no infinite factor in Equation XI.

[2] Disregarding the fact that the factor mentioned above can not be treated as small near the origin, the results may be considered as sufficiently accurate for all points beyond $x = 0.1$.

REPORT No. 383

ON THE THEORY OF WING SECTIONS WITH PARTICULAR REFERENCE TO THE LIFT DISTRIBUTION

PART III

DIRECT CALCULATION OF THE IDEAL ANGLE OF ATTACK

$$\alpha_I = -\frac{\epsilon_1+\epsilon_0}{2}$$

If the ϵ-curve is not found we may calculate α_I as follows: $\epsilon = -\Sigma A_n \cos n\theta$

$$-\epsilon_0 = +A_0+A_1+A_2+ \ldots .$$
$$-\epsilon_1 = A_0-A_1+A_2-A_3 \ldots$$
$$-(\epsilon_0+\epsilon_1) = 2(A_0+A_2+A_4+ \ldots .)$$
$$= 2\frac{2}{\pi}\int_0^\pi r d\theta(\sin 0\,\theta + \sin 2\,\theta + \ldots).$$

This is equal to the imaginary part of $\frac{4}{\pi}\int_0^\pi r\,d\theta \Sigma e^{in\theta}$ with $n=0, 2, 4, 6, \ldots,$

But $\Sigma e^{in\theta}$ $(n=0, 2, 4, 6, \ldots) =$

$$\frac{1}{1-e^{2i\theta}} = \frac{e^{-i\theta}}{e^{-i\theta}-e^{i\theta}} = \frac{\cos\theta - i\sin\theta}{-2i\sin\theta}$$

Therefore $-(\epsilon_0+\epsilon_1) = \frac{2}{\pi}\int_0^\pi r d\theta \cot\theta$

but $r = \frac{2y}{\sin\theta}$ and $d\theta = \frac{2dx}{\sin\theta}$

We obtain $-(\epsilon_0+\epsilon_1)$

$$= \frac{2}{\pi}\int_0^1 \frac{2y}{\sin\theta}\frac{2dx}{\sin\theta}\cot\theta = \frac{8}{\pi}\int_0^1 y dx \frac{\cos\theta}{\sin^3\theta}$$
$$= \frac{8}{\pi}\int^1 y dx \frac{1-2x}{8[x(1-x)]^{\frac{3}{2}}} = \frac{1}{\pi}\int_0^1 \frac{y dx(1-2x)}{[x(1-x)]^{\frac{3}{2}}}$$
$$\alpha_I = \frac{1}{2\pi}\int_0^1 \frac{y dx\,(1-2x)}{[x(1-x)]^{\frac{3}{2}}} = \frac{1}{2\pi}\int_0^1 \frac{y dx\,(1-2x)}{R^3}. \quad \text{XII}$$

A 4-point method gives the ideal angle in degrees, with sufficient accuracy as follows:

$$\alpha_I{}^0 = 623\ (y_1-y_5)+47\ (y_2-y_4)$$

where y_1, y_2, y_4, and y_5 are the ordinates of the mean camber line with respect to its chord at $x=0.542$, 12.574, 87.426, and 99.458 per cent chord, respectively.

PRESSURE DISTRIBUTION ON THE THIN WING AT $\alpha=\alpha_I$

Rearranging, we obtain easily from Equation VIII:

$$P = 4\sqrt{x(1-x)}\frac{d\epsilon}{dx} + \frac{2}{\sqrt{x(1-x)}}[2\alpha(1-x) + \epsilon_1 + \epsilon(1-2x)] \quad \text{XIII}$$

and with

$$\alpha_I = -\frac{\epsilon_0+\epsilon_1}{2}:$$

$$P_I = 4\sqrt{x(1-x)}\frac{d\epsilon}{dx} + \frac{2}{\sqrt{x(1-x)}}[-\epsilon_0(1-x) + 2\epsilon\left(\frac{1}{2}-x\right) + \epsilon_1 x]$$

or

$$P_I = 4\sqrt{x(1-x)}\frac{d\epsilon}{dx} + \frac{2}{\sqrt{x(1-x)}}[(-\epsilon_0+\epsilon) + (\epsilon_0-2\epsilon+\epsilon_1)x].$$

This pressure distribution may, in order to fix our thoughts, be termed the basic pressure distribution of the section.

Writing $\sqrt{x(1-x)} = R$, we have

$$P_I = 4R\frac{d\epsilon}{dx} + \frac{2}{R}[\epsilon - \epsilon_0 + (\epsilon_0 - 2\epsilon + \epsilon_1)x] \quad \text{XIV}$$

This is the exact expression for P at the ideal angle of attack for a thin airfoil. In this expression P_I is the pressure difference and ϵ the distortion at x, ϵ_0 and ϵ_1 are the values of ϵ at $x=0$ and at $x=1$, respectively. The equation is readily integrated and yields the value of the lift $L_I = \pi\ (\epsilon_1-\epsilon_0)$. The basic distribution curves for three airfoils are shown in Figures 21, 22, and 23. The comparison has for convenience been made at the same total lift.

It is noted that the center of lift of the measured distribution is nearer the leading edge than that of the theoretical distribution. It is believed that this effect is partly due to the finite aspect ratio of the airfoils on which the measurements were made. The exact effect of the finite aspect ratio is not simply to change the direction of flow as considered by the usual theory, but more precisely to change the local curvature in a certain prescribed manner. The flow near the leading edge is less affected by the "downwash" thus producing a lift which is greater than that based on the average direction of flow. Near the trailing edge the reverse is true.

The theory of thin wing sections must thus be based on the following assumptions:

I. The flow must leave the trailing edge smoothly (Kutta's condition).

II. The flow must enter the leading edge smoothly (front edge condition).

In all other cases the theory leads to infinite pressure differences.

The first condition requires a circulation

$$\Gamma = \pi V(\alpha + \epsilon_1),$$

while according to condition II, the angle of attack must be equal to

$$\alpha_I = -\frac{\epsilon_0 + \epsilon_1}{2}.$$

On basis of the theory developed above, we are actually able to explain certain properties of the lift curve. For instance, to obtain an efficient high lift wing section, it is obvious that ϵ_0 should be made large.

The circulation at this condition point (I and II satisfied) is equal to

$$\Gamma_I = \frac{1}{2}\pi V(\epsilon_1 - \epsilon_0) \text{ and the lift } L_I = \pi(\epsilon_1 - \epsilon_0). \quad \text{XV}$$

Note that both α_I and L_I are functions of the shape of the foil. It is impossible to devise a more efficient flow than that satisfying the above conditions.

Thickening the airfoil does not improve the condition. It only permits a certain violation of condition II with less disagreeable consequences. This fact

FIGURE 8

explains why the Munk theory, acknowledging solely condition I, gives better results when applied to thick airfoils, while the theory actually is developed for infinitely thin foils.

The fact is that the thickening of the foil makes it less efficient, but gives it a certain immunity against the losses caused by incorrect flow past the leading edge. This will be shown later.

The above deductions explain several facts relating to the shape of the lift curve. For instance, why the most efficient angle of incidence, in general, is greater for a section with a greater curvature at the leading edge. We know that the minimum friction loss clearly must be expected to occur near

$$\alpha = \alpha_I = -\frac{\epsilon_1 + \epsilon_0}{2}.$$

The entrance loss is evidently a function of $|\alpha - \alpha_I|$. The case is quite similar to that of the entrance loss in turbines. We may write for this loss

$$L = \beta \cdot |\alpha - \alpha_I|^{\eta}.$$

Experience has shown that η is very large for a sharp leading edge and that it decreases rapidly as the thickness of the airfoil is increased. It is, however, difficult to separate this loss experimentally.

CALCULATION OF EXPRESSION FOR THE BASIC LIFT

In analogy with the calculations for α_I we obtain:

$$\begin{aligned} \epsilon_1 &= -A_0 + A_1 - A_2 + \ldots \\ -\epsilon_0 &= \ \ A_0 + A_1 + A_2 + \ldots \\ \hline \epsilon_1 - \epsilon_0 &= 2A_1 + 2A_3 + \ldots = 2(A_1 + A_3 + A_5 + \ldots) \end{aligned}$$

$$\epsilon_1 - \epsilon_0 = \frac{4}{\pi}\int_0^{\pi} r\,d\theta(\sin\theta + \sin 3\theta + \ldots)$$

or the imaginary part of $\frac{4}{\pi}\int_0^{\pi} r\,d\theta \Sigma e^{in\theta}$ where $n = 1,3,5, \ldots$

but

$$\sum_{n\,odd} e^{in\theta} = \frac{e^{i\theta}}{1 - e^{2i\theta}} = \frac{1}{e^{-i\theta} - e^{i\theta}} = \frac{1}{-2i\sin\theta} = \frac{i}{2}\frac{1}{2\sin\theta}$$

and

$$\epsilon_1 - \epsilon_0 = +\frac{2}{\pi}\int_0^{\pi} r\,d\theta\,\frac{1}{\sin\theta} = +\frac{2}{\pi}\int_0^1 \frac{1}{\sin\theta}\frac{2y}{\sin\theta}\frac{2dx}{\sin\theta}$$

$$= +\frac{8}{\pi}\int_0^1 \frac{y\,dx}{\sin^3\theta} = +\frac{1}{\pi}\int_0^1 \frac{y\,dx}{[x(1-x)]^{\frac{3}{2}}}$$

and

$$L_I = \int_0^1 \frac{y\,dx}{[x(1-x)]^{\frac{3}{2}}} = \int_0^1 \frac{y\,dx}{R^3}. \quad \text{XVa}$$

The approximate Gauss' method gives: $L_I = 69(y_1 + y_5) + 6.8(y_2 + y_4) + 3.6y_3$ where y_3 is taken at $x = 50$ per cent C.

This function has considerable significance as being the lift at the ideal angle of attack, or the lift of the wing when the flow is theoretically correct around the leading edge.

It is noticed how the elements near front and rear are of the greatest importance.

From Equation XVa we obtain

$$\int_0^{\Delta x} \frac{y'\Delta x}{\Delta x^{\frac{3}{2}}}dx = y'\int_0^{\Delta x}\frac{dx}{\Delta x^{\frac{1}{2}}} = +2y'\Delta x^{\frac{1}{2}}.$$

This expression shows that in order to obtain a high basic lift the angle near the nose should be steep. The fact that x appears only in ½ power, shows that the steepness need not extend for any length. In fact, the best airfoil would be the one shown in Figure 8 if it were not for the fact that we must maintain potential flow. Experience shows that any great curvature near the rear edge is poor aerodynamically. It is also in contradiction with the requirement of a small center of pressure travel.

ADDITIONAL PRESSURE WHEN THE ANGLE OF INCIDENCE IS DIFFERENT FROM THE IDEAL ANGLE

We will observe from the expression for the pressure distribution, Equation XIII, that the increase in the pressure due to a change in the angle α is equal to

$$\frac{4}{\sqrt{x(1-x)}}(\alpha - \alpha_1)(1-x) \text{ or}$$

$$P_a = 4\sqrt{\frac{1}{x} - 1}\,(\alpha - \alpha_I) = 4\frac{R}{x}(\alpha - \alpha_I). \quad \text{XVI}$$

The expression is, as pointed out, obviously far from giving the physical facts.

The infinite pressure, of course, does not occur. In the limiting case sound velocity is reached, while the other extreme corresponds to a velocity of zero at the stagnation point. These facts are neglected in the present theory.

If the angle of attack is different from α_I we will now consider what actually takes place near the nose. We restrict ourselves to velocities considerably less than the velocity of sound.

The velocity of potential flow near the surface of a circle is given by the expression:

$$\frac{dw}{dz} = -2iVe^{i\phi}\left[\sin(\alpha+\Phi)+\frac{K}{4\pi aV}\right].*$$

Let the rear stagnation point occur at $\Phi=\pi$.
This condition is satisfied by:

$$\frac{dw}{dz} = -2iVe^{i\phi}\,[\sin(\alpha+\Phi)+\sin\alpha].$$

For small values of α and Φ we write:

$$\frac{dw}{dz} = -2iVe^{i\phi}\,(2\alpha+\Phi) \text{ and } \left|\frac{dw}{dz}\right| = 2V(2\alpha+\Phi).$$

Let us transform this circle into an ellipse:

$$\zeta = z+\frac{a^2}{z}\beta.$$

We have then

$$\frac{d\zeta}{dz} = 1-\frac{a^2}{z^2}\beta$$

$$\frac{d\zeta}{dz} = 1-\frac{a^2}{a^2}\beta(\cos 2\Phi - i\sin 2\Phi)$$

$$\frac{d\zeta}{dz} = 1-\beta(\cos 2\Phi - i\sin 2\Phi)$$

For small values of Φ

$$\frac{d\zeta}{dz} = 1-\beta(1-2i\Phi),$$

neglecting quantities of higher order than the first.
Further:

$$\left|\frac{d\zeta}{dz}\right|^2 = (1-\beta)^2+(2\Phi\beta)^2.$$

This gives for the square of the velocity near $\Phi=0$

$$w^2 = 4V^2\,\frac{(2\alpha+\Phi)^2}{(1-\beta)^2+(2\Phi\beta)^2}$$

With β close to unity, we may write:

$$w^2 = 4V^2\,\frac{(2\alpha+\Phi)^2}{(1-\beta)^2+4\Phi^2} = V^2\frac{(2\alpha+\Phi)^2}{\left(\frac{1-\beta}{2}\right)^2+\Phi^2}.$$

This expression gives the square of the velocity near the front edge of a flat elliptical cylinder inclined at an angle α toward the direction of flow at infinity and equipped with a circulation sufficient in magnitude to locate the rear stagnation point at the corresponding end point of the major axis. The flow is indicated schematically in Figure 9. Reshaping of the rear part of this section so as to simulate a flat airfoil does not materially alter the flow at the front edge.

It may be shown that:

$$\frac{\rho}{4a} = \frac{(1-\beta)^2}{8} \text{ or } \frac{\rho}{c} = \frac{1}{2}\left(\frac{1-\beta}{2}\right)^2$$

where ρ is the radius of curvature at the nose and c the chord.

Consequently:

$$w^2 = V^2\,\frac{(2\alpha+\Phi)^2}{\frac{2\rho}{c}+\Phi^2}.$$

We are more interested in the difference between the pressures at the upper and lower side of the nose.

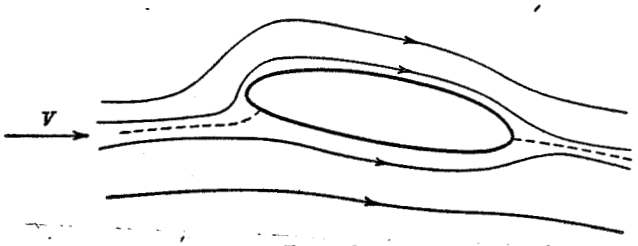

FIGURE 9

The pressure at Φ differs from the total pressure by

$$P_1 = \frac{(2\alpha+\Phi)^2}{\frac{2\rho}{c}+\Phi^2}$$

and at $-\Phi$ by

$$P_2 = \frac{(2\alpha-\Phi)^2}{\frac{2\rho}{c}+\Phi^2}.$$

The difference is

$$P = \frac{8\alpha\Phi}{\frac{2\rho}{c}+\Phi^2} \qquad \text{XVII}$$

This function has a maximum at $\Phi^2=\frac{2\rho}{c}$.

This maximum equals

$$P_{max} = 4\frac{\alpha}{\sqrt{\frac{2\rho}{c}}} \text{ or referred to the ideal angle } P_m$$

$$= 4\frac{(\alpha-\alpha_I)}{\sqrt{\frac{2\rho}{c}}}. \qquad \text{XVIII}$$

It may be shown that the point of the airfoil corresponding to $\Phi^2=\frac{2\rho}{c}$ is located at $x=\frac{\rho}{2}$ or at the *focal point of the ellipse.*

It will be understood that the local flow very close to the nose is not very dependent on the shape of the rear part of the foil, provided the Kutta condition is satis-

* *(Reference 1, equation 10.)*

fied; that is, that the flow leaves the circle at $\Phi=\pi$ as prescribed above.

The greatest pressure difference across the nose thus occurs at a point midway between the center of curvature and the front edge.

Its magnitude equals

$$P_{max}=4\frac{\alpha-\alpha_I}{\sqrt{\frac{2\rho}{c}}}.$$

It will be noticed that the point is usually located less than 1 per cent from the edge and that the magnitude of this pressure difference for ordinary airfoils is usually less than $4q$ except at the highest angles of attack. (Table VI.)

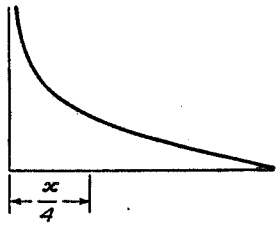

FIGURE 10

In addition to the basic pressure distribution at α_I given in equation XIV, we must add the distribution due to the difference in the angle of attack. The latter can be obtained as follows: For points near $x=0$, we employ Equation XVII and for points near $x=1$, we employ Equation XVI. By applying our analysis to a straight Joukowsky section, we find further that no great change in the lift per radian takes place. That is, the concentrated lift at the nose of a thin section will appear as a distributed lift of approximately the same magnitude. The center of this lift will then move from the 25 per cent location to a somewhat greater value of x. In plotting the curve, we will consider it sufficiently accurate for most purposes to determine P_{max} (Equation XVIII) at $x=\frac{\rho}{2}$ and to draw the line as indicated in Figure 24. The area or total lift per radian obtained in this manner is less than 2π and almost exactly equal to the observed values. An expected increase of lift along the remainder of the airfoil is, for practical purposes, almost completely nullified by the frictional losses, Table VI and Figure 25.

The total lift of an airfoil is then mathematically expressed as:

$$L=L_I+a_o\ (\alpha-\alpha_I) \qquad \text{XIX}$$

There exists a slight increase in this coefficient a_0 with a decrease of the radius of curvature at the front edge (see Figure 25). It thus probably serves no purpose to refine the above simple method by considering second-order terms or departures from an elliptical nose.

EXPRESSION OF MOMENT ON THE AIRFOIL

We are on basis of the theory here represented able to furnish a clear picture of the question of the center of pressure travel. The total moment is represented by: (1) The moment of the basic distribution and (2) the moment of the additional distribution.

The center of pressure of the additional distribution is for the thin airfoil located at $x=0.25$ and for a conventional airfoil (and potential flow) say, at $x=0.30$.

The magnitude of the travel of the center of pressure thus depends on the basic lift and on the moment of the basic lift about this point.

The magnitude of this moment M equals:

$$\int_0^1 P_1(x-0.25)\mathrm{d}x$$

$$=-\int_0^1 4x\mathrm{d}x\frac{\mathrm{d}}{\mathrm{d}x}\left[(\epsilon_1-\epsilon)\sqrt{x(1-x)}\right]$$

$$=-\int_0^1 4x\mathrm{d}\left[(\epsilon_1-\epsilon)\sqrt{x(1-x)}\right].$$

It may be written

$$-\left[4x(\epsilon_1-\epsilon)\sqrt{x(1-x)}\right]_0^1+\int_0^1 4(\epsilon_1-\epsilon)\sqrt{x(1-x)}\mathrm{d}x$$

or

$$M=4\int_0^1(\epsilon_1-\epsilon)\sqrt{x(1-x)}\mathrm{d}x=4\int_0^1(\epsilon_1-\epsilon)R\mathrm{d}x \qquad \text{XX}$$

This integral is, in general, positive due to the fact that ϵ_1 ordinarily is the greatest value of ϵ. (See fig. 5.)

Any great accuracy in the total moment serves no particular purpose. The center of pressure of the additional distribution is actually located near $x=0.3$,

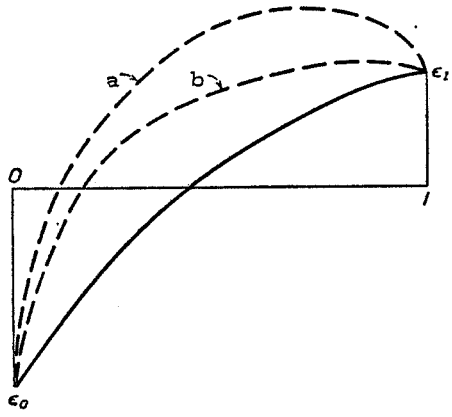

FIGURE 11

however, and the actual moment of the basic lift then differs slightly from Equation XX.

The simple derivation of the above moment in accordance with the present theory is, however, a distinct advantage, and peculiarly enough, the center of pressure of the additional distribution actually tends to shift forward, due to the effect of the finite aspect ratio.

It is interesting to know what happens if we keep the end values fixed at ϵ_0 and ϵ_1, but decrease the area $\epsilon_1-\epsilon$. This is indicated by the two dotted lines a and b in Figure 11.

M is decreased, decreasing with it the travel of the center of pressure. Curve a corresponds to $M=0$

with a fixed center of pressure, b to a small M and small travel of the center of pressure.

The corresponding appearance of the airfoils is given in Figures 12 and 13. Figure 12 corresponds to the curve a with $M=0$. S shape is necessary as

FIGURE 12

shown by Munk. The integral contains in this case a sufficient number of negative elements.

Negative elements are avoided in curve b where ϵ is stationary for a considerable distance from the rear end. This leads to the foil shown in Figure 13, with

FIGURE 13

a straight rear end inclined at a fixed angle β. We know from experience that it is quite difficult to maintain potential flow along the upper side of an airfoil if the change of direction is abrupt. For this reason the foil in Figure 13 with no change in curvature is probably superior to the one shown in Figure 12.

THE IDEAL AIRFOIL

We keep in mind that we do not want any large change in the location of the center of pressure. The

FIGURE 14

foil arrived at so far should look like the one shown in Figure 14.

It is evident from the preceding analysis that α_I and L_I should correspond to the coefficients at cruising speed or at the speed for which the greatest efficiency is desired. With a well-rounded front edge the importance of the front edge requirement is lessened, but not removed. The well-known poor characteristics of an airfoil approaching the mathematically

FIGURE 15

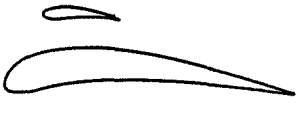

FIGURE 16

"thin" section is due to this cause, as has been pointed out. It may be expected that the thin section at the optimum angle of attack α_I in a flow without great initial turbulence is the best of all airfoils.

But even for thick airfoils this consideration must be given proper attention. We must give as little occasion as possible for the creation of disturbances near the front edge. The study of the airplane nose is thus a problem of considerable importance. The design shown in Figure 15 will permit a large "most efficient" lift as far as the entrance condition is concerned. It leads, however, to a great curvature of the upper surface of the foil of conventional thickness. We know from experience that such designs

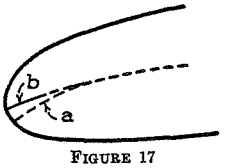

FIGURE 17

cause premature turbulence. It is pointed out that a great increase in maximum lift above that of the conventional airfoil might be obtained by a foil of the above proposed type in conjunction with an auxiliary deflecting plate or guiding vane, located above the

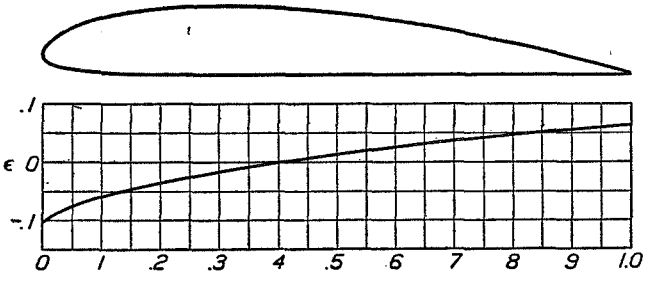

FIGURE 18.—Distortion ϵ. Clark Y airfoil

point of the upper surface having the greatest ordinate, as indicated in Figure 16. This scheme has little justification or value in conjunction with airfoils of conventional designs. It is hoped, however, that such design might lead to a thicker and narrower

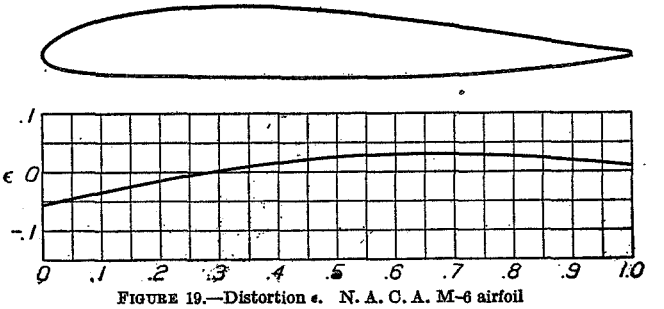

FIGURE 19.—Distortion ϵ. N. A. C. A. M-6 airfoil

main wing section, which is sometimes desirable for structural reasons.

AUTOMATIC ADJUSTMENT OF THE ENTRANCE ANGLE

If a "thin" wing section should be employed successfully as an airfoil, it would at least be necessary to have the leading edge adjustable. The importance of the angle at the very edge has been pointed out before. This end has unconsciously been obtained by rounding the front edge. This is equivalent to permitting change in the entrance angle and thus in the very shape of the foil. To make this point clear we refer to Figure 17, where b is the "shape" of the

airfoil at low angles of attack and a at high angles. It should be pointed out that the actual "edge" of

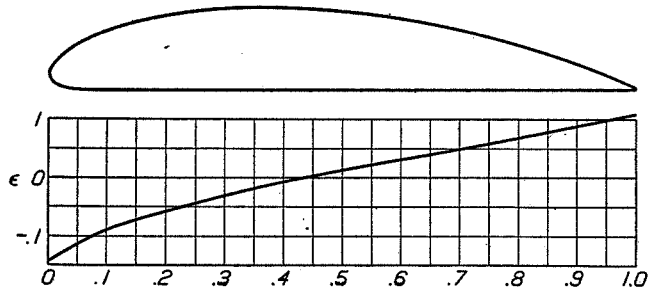

FIGURE 20.—Distortion ε. N. A. C. A. 84 airfoil

the section and of the associated "thin" section is the momentary location of the stagnation point. A

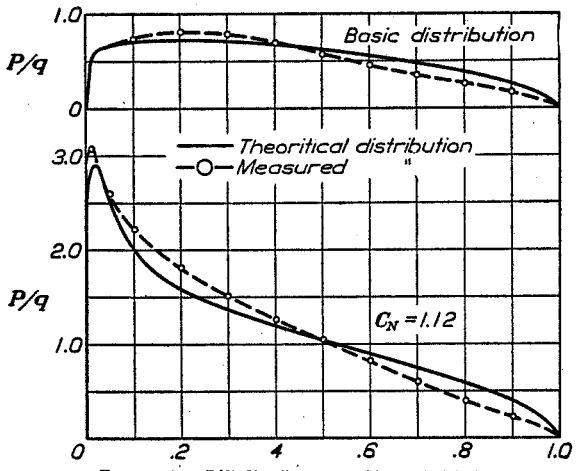

FIGURE 21.—Lift distribution. Clark Y airfoil

thick nose is thus virtually equivalent to an adjustable front edge. The thicker the section the greater is the possible change in the shape of the foil. That is,

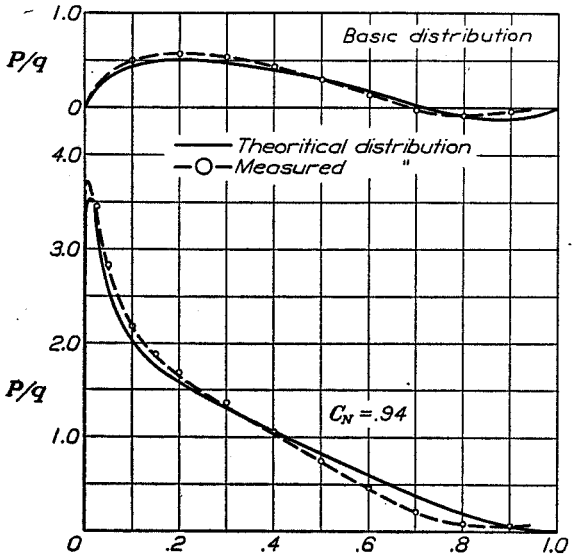

FIGURE 22.—Lift distribution. N. A. C. A. M-6 airfoil

the efficiency curve is flattened. The thin section on the other hand does not lend itself to any such "flexibility," hence its poorer characteristics.

The thickness of the foil beyond the nose is undesirable aerodynamically, since it causes a certain in-

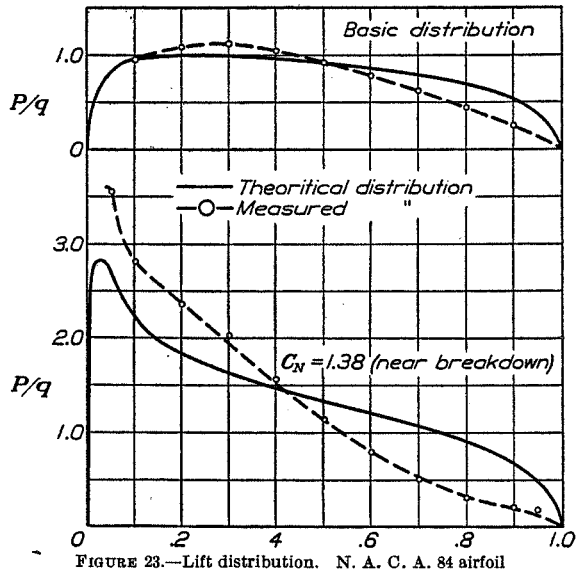

FIGURE 23.—Lift distribution. N. A. C. A. 84 airfoil

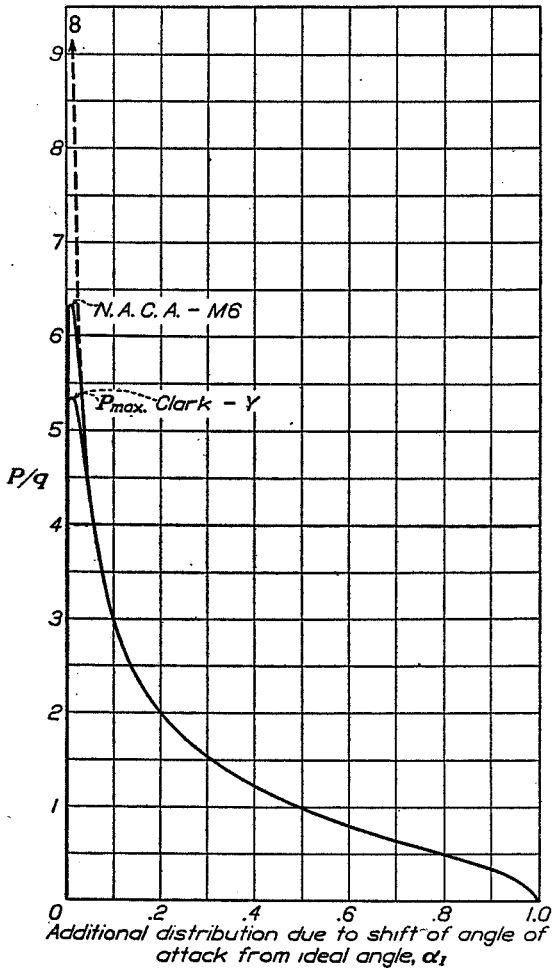

FIGURE 24.—Additional distribution

$$P_m = \frac{4(\alpha-\alpha_1)q}{\sqrt{\frac{2\rho}{c}}} \quad \left(at\ x = \frac{\rho}{2}\right)$$

Note: $P = 4\frac{R}{x}(\alpha-\alpha_p)q$. Ordinates are equal to P/q for $\alpha-\alpha_1=\frac{1}{4}$ rad.

crease in the fluid velocity on both sides of the foil. The least resistance is, however, introduced if a

fish-shaped section is used in conjunction with the desired type of nose. The pressure distribution at zero angle of a foil similar in shape to the wing section as regards thickness, but with no curvature of the mean ordinate, may be determined in conjunction with the testing of each foil.

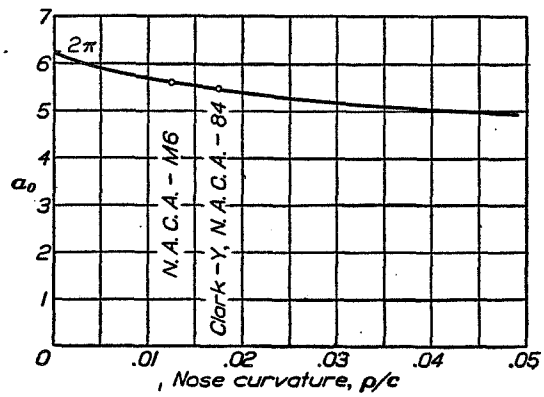

FIGURE 25.—Slope of the lift curve

SUMMARY OF NEW FORMULAS

With $R=\sqrt{x(1-x)}$, $q=1$

and the x-axis coinciding with the chord of the mean camber line.

$$e_{x_1}=\frac{1}{\pi}\int_0^1 \frac{y\,dx}{(x_1-x)\,R} \qquad (\Delta\epsilon_0=-2.85y_{0\text{-}05}\ \Delta\epsilon_1=2.85y_{0\text{-}95})$$

$$\alpha_I=-\frac{\epsilon_0+\epsilon_1}{2}=\frac{1}{2\pi}\int_0^1 \frac{y\,dx(1-2x)}{R^3}$$

$\alpha_I{}^0=623\ (y_1-y_5)+47(y_2-y_4)$ degrees where y_1, y_2, y_4, and y_5 are taken at $x=0.542$, 12.574, 87.426, and 99.458 per cent chord. (α_I is measured with respect to the chord of the mean camber line.)

$$P_I=4R\frac{d\epsilon}{dx}+\frac{2}{R}[\epsilon-\epsilon_0+(\epsilon_0-2\epsilon+\epsilon_1)x] \text{ lift intensity at } \alpha=\alpha_I$$

$$P_a=4\frac{R}{x}(\alpha-\alpha_I) \text{ additional lift valid for } x>0.1.$$

$$P_m=4\frac{\alpha-\alpha_I}{\frac{2\rho}{c}} \text{ maximum lift occurring at } x=\frac{\rho}{2}$$

$$M=4\int_0^1(\epsilon_1-\epsilon)R\,dx \text{ moment at } x=\frac{1}{4}$$

$$L_I=\pi(\epsilon_1-\epsilon_0)=\int_0^1\frac{y\,dx}{R^3} \qquad (\Delta L_I=2y'\,\Delta x^{\frac{3}{2}}) \text{ ideal lift.}$$

$$L_I=69(y_1+y_5)+6.8(y_2+y_4)+3.6y_3$$

where y_3 is the ordinate at $x=50$ per cent chord.

LANGLEY MEMORIAL AERONAUTICAL LABORATORY,
NATIONAL ADVISORY COMMITTEE FOR AERONAUTICS,
LANGLEY FIELD, VA., *November 14, 1930.*

REFERENCES

1. Glauert, H.: A Theory of Thin Airfoils. British A. R. C. Reports and Memoranda No. 910. February, 1924.

TABLE I

VALUES OF $R=\sqrt{x(1-x)}$

x	R	$1-x$	x	R	$1-x$
0.00	0.000	1.00	0.20	0.400	0.80
.01	.099	.99	.25	.433	.75
.02	.140	.98	.30	.458	.70
.03	.171	.97	.35	.477	.65
.04	.196	.96	.40	.490	.60
.05	.218	.95	.45	.497	.55
.10	.300	.90	.50	.500	.50
.15	.357	.85			

TABLE II

ANGULAR DISTORTION FOR THREE AIRFOILS

x	ϵ			x	ϵ		
	N.A.C.A. 84	Clark Y	N.A.C.A. M-6		N.A.C.A. 84	Clark Y	N.A.C.A. M-6
0.0	----------	----------	----------	0.4	−.007	−.001	+.015
.0125	----------	----------	----------	.5	----------	+.013	.025
.025	----------	−0.088	−0.052	.6	+.031	.025	----------
.05	−0.115	−.075	−.047	.7	----------	.036	.029
.075	----------	----------	----------	.8	.068	.046	.026
.1	−.090	−.059	−.035	.9	.089	----------	----------
.15	----------	----------	----------	.95	.099	.059	.014
.2	−.058	−.035	−.014	1.0	----------	----------	----------
.3	----------	−.016	----------				

TABLE III

BASIC DISTRIBUTIONS FOR THREE AIRFOILS

x	P_I Ordinates			x	P_I Ordinates		
	N.A.C.A. 84	Clark Y	N.A.C.A. M-6		N.A.C.A. 84	Clark Y	N.A.C.A. M-6
0.0	0.000	0.000	0.000	0.5	0.908	0.592	0.292
.0125	.478	.509	.170	.6	.830	.537	.169
.025	.649	.624	.214	.7	.785	.464	.016
.05	.847	.653	.311	.8	.679	.359	−.081
.075	.940	.679	.376	.9	.532	.243	−.115
.1	.952	.701	.424	.95	.386	.170	−.097
.15	.937	.698	.479	1.0	.000	.000	.000
.2	.995	.695	.510	Integrated lift	.804	.526	.206
.3	.991	.706	.462				
.4	.958	.653	.403				

TABLE IV

IDEAL ANGLE OF ATTACK AND IDEAL LIFT

	N. A. C. A. M-6	Clark Y	N. A. C. A. 84
Angle of zero lift	−0.5°	−5.5°	−7.5°
Ideal angle of attack (α_I)	1.4°	−.7°	−.3°
Ideal lift at α_I (L_I)	.208	.524	.798

NOTE.—Above angles are measured from the regular chord.

TABLE V

ADDITIONAL DISTRIBUTION FOR $x>0.1$

$R=\sqrt{x\,(1-x)}$

x	$\frac{R}{x}$	x	$\frac{R}{x}$	x	$\frac{R}{x}$
0.0	∞	0.15	2.38	0.7	0.654
.0125	8.88	.2	2.00	.8	.500
.025	6.24	.3	1.53	.9	.333
.05	4.36	.4	1.22	.95	.230
.075	3.52	.5	1.00	1.0	.0
.1	3.00	.6	.817		

TABLE VI

PRESSURE NEAR THE LEADING EDGE AND COEFFICIENT OF LIFT

CLARK Y

$\rho = 0.0175c$

$P_{max.} = 4\frac{1}{\sqrt{0.0350}}q = 5.34\,x\,4\,q$ (per radian) $(x=0.0088)$

$a_0 = 5.48$

N. A. C. A. M-6

$\rho = 0.0125c$

$P_{max.} = 4\frac{1}{\sqrt{0.0250}}q = 6.33\,x\,4\,q$ (per radian) $(x=0.0058)$

$a_0 = 5.60$

N. A. C. A. 84

$\rho = 0.0175c$

$P_{max.} = 4\frac{1}{\sqrt{0.0350}}q = 5.34\,x\,4\,q$ (per radian) $(x=0.0088)$

$a_0 = 5.48$

U. S. GOVERNMENT PRINTING OFFICE: 1931

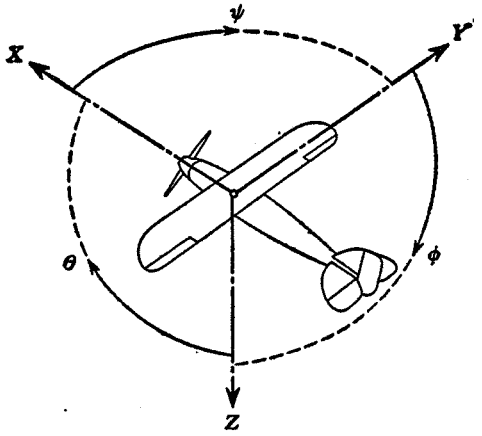

Positive directions of axes and angles (forces and moments) are shown by arrows

Axis		Force (parallel to axis) symbol	Moment about axis			Angle		Velocities	
Designation	Symbol		Designation	Symbol	Positive direction	Designation	Symbol	Linear (component along axis)	Angular
Longitudinal	X	X	rolling	L	$Y \longrightarrow Z$	roll	ϕ	u	p
Lateral	Y	Y	pitching	M	$Z \longrightarrow X$	pitch	θ	v	q
Normal	Z	Z	yawing	N	$X \longrightarrow Y$	yaw	ψ	w	r

Absolute coefficients of moment

$$C_l = \frac{L}{qbS} \qquad C_m = \frac{M}{qcS} \qquad C_n = \frac{N}{qbS}$$

Angle of set of control surface (relative to neutral position), δ. (Indicate surface by proper subscript.)

4. PROPELLER SYMBOLS

D, Diameter.
p, Geometric pitch.
p/D, Pitch ratio.
V', Inflow velocity.
V_s, Slipstream velocity.
T, Thrust, absolute coefficient $C_T = \frac{T}{\rho n^2 D^4}$
Q, Torque, absolute coefficient $C_Q = \frac{Q}{\rho n^2 D^5}$
P, Power, absolute coefficient $C_P = \frac{P}{\rho n^3 D^5}$.
C_s, Speed power coefficient $= \sqrt[5]{\frac{\rho V^5}{P n^2}}$.
η, Efficiency.
n, Revolutions per second, r. p. s.
Φ, Effective helix angle $= \tan^{-1}\left(\frac{V}{2\pi r n}\right)$

5. NUMERICAL RELATIONS

1 hp = 76.04 kg/m/s = 550 lb./ft./sec.
1 kg/m/s = 0.01315 hp
1 mi./hr. = 0.44704 m/s
1 m/s = 2.23693 mi./hr.

1 lb. = 0.4535924277 kg
1 kg = 2.2046224 lb.
1 mi. = 1609.35 m = 5280 ft.
1 m = 3.2808333 ft.